Self-purification in Si nanocrystals: An energetics study

Tzu-Liang Chan,[1,2] Hyunwook Kwak,[1,3] Jae-Hyeon Eom,[1] S. B. Zhang,[2] and James R. Chelikowsky[1,4]
[1]*Center for Computational Materials, Institute for Computational Engineering and Sciences, University of Texas, Austin, Texas 78712, USA*
[2]*Department of Physics, Applied Physics, and Astronomy, Rensselaer Polytechnic Institute, Troy, New York 12180, USA*
[3]*Applied Sciences Laboratory, Institute for Shock Physics, Washington State University, Spokane, Washington 99202, USA*
[4]*Departments of Physics and Chemical Engineering, University of Texas, Austin, Texas 78712, USA*
(Received 21 December 2009; revised manuscript received 9 August 2010; published 10 September 2010)

We examine the energetics of dopants in Si nanocrystals to understand the phenomena of "self-purification," i.e., a process by which extrinsic defects in the interior of a nanocrystal are expelled to the surface. Specifically, we calculate the changes in the total energy of a dopant atom in a Si nanocrystal with respect to position. We consider typical dopant atoms such as P, B, and Li. We find these dopants exhibit different variations in total energies as they move from the center toward the surface of a nanocrystal. These differences can be explained by the change in electronic binding energy and the interaction of the dopant with the surface, i.e., the interaction of a dopant-induced strain with the nanocrystal surface energy.

DOI: 10.1103/PhysRevB.82.115421 PACS number(s): 73.21.La, 71.15.Mb

I. INTRODUCTION

Bulk semiconductors can be functionalized by introducing impurities or dopants into a host material. For example, dopants can create charge carriers in semiconductor for electronic devices. Similarly, magnetic atom impurities can create dilute magnetic semiconductors for spintronic devices. However, doping semiconductor nanomaterials can be complex and our understanding of these materials is problematic. This lack of understanding can pose significant obstacles in fabricating semiconductor devices at nanoscale.

Typical doping concentration in bulk materials is $10^{13}-10^{18}$ cm^{-3}. This roughly corresponds to 1 dopant atom per 10 000 to 1 billion Si atoms. A Si nanocrystal of a few nanometers in diameter may contain only a few hundred to a few thousand Si atoms. As such, the introduction of just one impurity atom into a nanocrystal can result in many orders of magnitude higher impurity concentration than for the typical doping in macroscopic crystals. Indeed, a "self-purification" phenomenon has been observed experimentally where it is nearly impossible to incorporate magnetic Mn dopants into ZnSe and CdSe nanocrystals, whereas Mn has a high solubility for the macroscopic counterparts.[1,2]

There are several theories for self-purification mechanisms. Previous work[3–6] considered the heat of formation of introducing an impurity into a nanocrystal. By studying heats of formation as a function of nanocrystal size, it was observed that a thermodynamic driving force could aid in the expulsion of the impurity atom from a nanomaterial.[3–6] A different point of view is to consider the nucleation process during synthesis in experiments.[2] If an impurity atom can reside on the surface of a nanocrystal long enough, further nucleation and growth of the nanocrystal will incorporate the impurity inside. Otherwise, the impurity will be absent during the nanocrystal growth. The binding energy of the impurity atom on the nanocrystal surface can be used as a measure of how long the atom can stay on the surface. A higher binding energy indicates that the nanocrystal has a higher probability to be formed with the impurity. However, even if an impurity can be incorporated into a nanocrystal, there is a second driving force to self-purify the core of a nanocrystal, i.e., we have shown that impurity diffusion can be substantially faster within a nanocrystal at experimental synthesis temperature compared to bulk materials. The favorable energetics of placing an impurity near the surface plus large kinetic factors such as a large diffusion constant, and a short diffusion path to a surface, will effectively purge impurity atoms from the nanocrystal interior.[7]

Here, we will examine the total energy of a doped Si nanocrystal as a function of dopant position. We will find that different dopants exhibit different trends in total energy as they move within a nanocrystal. We will then elucidate why some dopants have the lowest energy at the surface leading to self-purification while others may behave differently. We express the total-energy variation in a dopant within a nanocrystal into two different contributions: an electronic binding-energy term which can be understood using a hydrogenic model and a surface term which has a strain contribution. In order to understand the physics of the two contributions, we compare P, B, and Li in Si nanocrystals. P and B are typical *n*-type and *p*-type dopants in Si, respectively, and Li is an interstitial defect that has been recently used in high capacity energy storage in Si nanostructures.[8] Compared to previous studies on this subject, our work goes beyond a qualitative argument and establishes a quantitative framework for understanding the energetics of dopants in nanomaterials.

II. COMPUTATIONAL DETAILS

Our calculations are based on density-functional theory[9,10] using a real-space grid code PARSEC.[11–13] The PARSEC code solves the self-consistent Kohn-Sham equation by using damped Chebyshev polynomial filtered subspace iteration, which can avoid repeatedly diagonalizing the Hamiltonian during self-consistent iterations.[14,15] The local spin-density approximation as determined by Ceperley-Alder[16] and parametrized by Perdew-Zunger[17] is used for the exchange-

correlation functional. The real-space grid is 0.4 a.u. The convergence test of the grid spacing is done by calculating the difference in total energy between two doped Si nanocrystals, which differ only by the dopant position. The difference in total energies is converged to within 0.01 eV. Such test is carried out for P, B, and Li individually.

The ionic potentials are replicated using Troullier-Martins pseudopotentials[18] in the Kleinman-Bylander form.[19] Cut-off radii for the s, p, and d components of the P pseudopotential are chosen to be 1.8 a.u., 1.8 a.u., and 3.2 a.u. (1 a.u. $=0.529$ Å) respectively, Si has 2.7 a.u. and 3.8 a.u. for the s and p components, Li has 2.4 a.u. for both the s and p components, and H has 2 a.u. for its s component. The cut-off radii for the B pseudopotential is the same as that of P but without the d component. The p component is chosen to be the local part of the Kleinman-Bylander form for Si and P while s is the local part for Li, B, and H. All the pseudopotentials are generated using ground-state electronic configurations.

Our Si nanocrystals adopt a bulk diamond structure and roughly spherical in shape in accordance with experimental observation.[20] The nanocrystals have both $\langle 111 \rangle$ and $\langle 100 \rangle$ facets which have the lowest surface energies. The surface dangling bonds are passivated by hydrogen atoms to remove the surface states from the energy gap. The experimentally synthesized Si nanocrystals are usually embedded in an amorphous silicon dioxide matrix. While the Si/SiO_2 interface is in general not the same as hydrogen passivation, all the dangling bonds of the Si surface are passivated by the oxide.[21] Hence, both types of interface serve the role of saturating the dangling bonds on the surface.

A spherical domain encloses the Si nanocrystal and confined boundary condition is imposed on the domain boundary at which the wave function is set to zero. There is a vacuum space of 8 a.u. between the surface of the nanocrystal and the domain boundary which is sufficient to converge the total energy of the system. The initial atomic structure for each calculation is slightly perturbed from its ideal bulk geometry to allow the system to relax to the appropriate symmetry and all the structures are optimized till the force on each atom is less than 0.001 Ry/a.u.

III. THEORY

We calculate the change in total energy as the dopant atom moves from the center of a Si nanocrystal toward the surface. For Li, the energetically stable positions are the interstitial tetrahedral sites [see Fig. 1(c)]. We move the Li atom from the center tetrahedral position toward a tetrahedral site close to the surface along the [110] direction. For P and B dopants, we substitute a Si atom as these dopants are known to be substitutional in bulk Si.[22] Specifically, we substitute different Si atoms in a nanocrystal along the [110] direction. [110] is chosen for convenience as it is along the $+x$ direction as illustrated in Fig. 4(a). All the dopant atoms are required to move along this direction for comparison. We avoid P and B substituting Si atoms that are bonded to H.

The change in total energy relative to a doped Si nanocrystal with the dopant at the center is

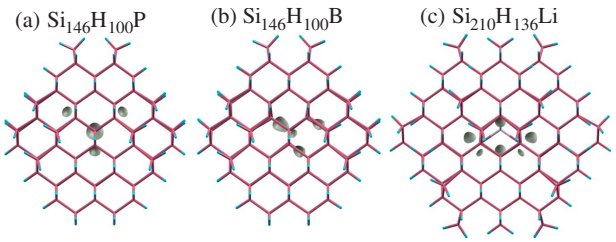

FIG. 1. (Color online) A surface contour plot of the defect wave function for a (a) P-, (b) B-, and (c) Li-doped Si nanocrystals. The dopant atom is at the center of each Si nanocrystal. For clarity, only the interatomic bonds are drawn.

$$\Delta E_i = E_i - E_0, \tag{1}$$

where the subscript i denotes the distance between the dopant and the origin [see Fig. 4(a) for an illustration]. The subscript 0 means that the dopant is at the center of the Si nanocrystal. For donors Li and P, by adding and subtracting E_i^+ and E_0^+ (the superscript + indicates that the nanocrystal is ionized by removing an electron) in the above equation, we obtain

$$\begin{aligned} \Delta E_i &= (E_i^+ - E_0^+) - \{(E_i^+ - E_i) - (E_0^+ - E_0)\} \\ &= \Delta E_i^+ - (IE_i - IE_0) = \Delta E_i^+ - \Delta IE_i \\ &= \Delta E_i^+ - \Delta BE_i. \end{aligned} \tag{2}$$

IE is the ionization energy of a doped Si nanocrystal. The last equality follows by noting that the binding energy of the defect electron can be evaluated using ΔSCF (Ref. 23) by

$$BE_i = IE_i - EA, \tag{3}$$

where EA is the electron affinity of a pure Si nanocrystal with the same size as the doped nanocrystal. Since EA is independent of the dopant position, ΔIE_i is the same as ΔBE_i. For acceptors, a similar expression as Eq. (2) can be derived by adding and subtracting E_i^- and E_0^- to ΔE_i instead,

$$\Delta E_i = \Delta E_i^- - \Delta BE_i. \tag{4}$$

Within simple effective-mass theory, a Si nanocrystal can be regarded as a dielectric sphere, and the dopant atom represents a positive ion for Li and P donors or a negative ion for a B acceptor embedded inside the dielectric. The defect electron (for donor) or hole (for acceptor) and the ion form a hydrogenic system. Equations (2) and (4) say that the energy change in the hydrogenic system with position can be split into two parts. ΔE^+ (ΔE^-) is the change in total energy when moving an ionized defect atom toward the surface, and is related to the effect of the surface (for example, the chemistry and the polarization induced by the passivating atoms) and defect-induced strain as we will see later. ΔBE is the change in binding energy of the electron (hole) as the ion changes position. Since the electronic binding energy and strain contribute to the change in total energy, we will examine the defect wave functions and the distribution of strain in doped Si nanocrystals in the following sections. In this study, we focus only on the difference in behavior between different dopants and keep the H passivation the same.

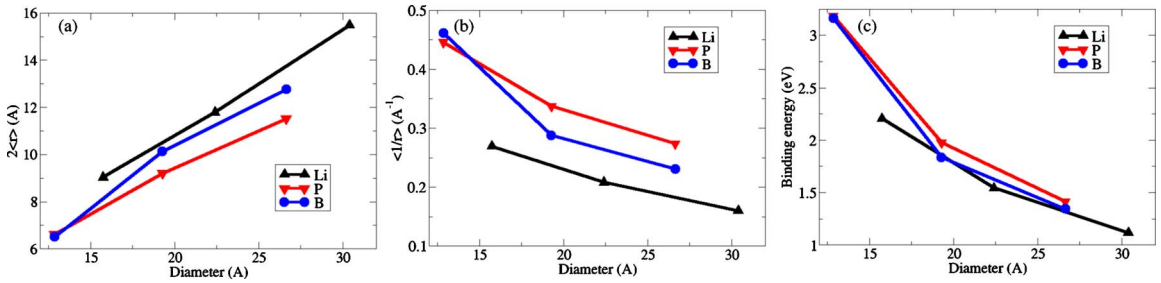

FIG. 2. (Color online) (a) The size of the defect wave function ($2\langle r\rangle$), (b) a measure of the Coulomb interaction between the dopant ion and the defect electron/hole ($\langle 1/r\rangle$), and (c) the electronic binding energy of a doped Si nanocrystal as a function of nanocrystal size. For each size, the dopant atom is located at the center of the nanocrystal.

A. Characterization of defect wave function

For a doped Si nanocrystal, there is an eigenstate inside the energy gap when compared to the eigenvalue spectrum of a pure Si nanocrystal having the same size. The state is related to the defect atom as we will see below, therefore we refer it as the defect wave function. Figure 1 illustrates the shape of the wave function with the dopant at the center of a doped Si nanocrystal. For P, the defect wave function has its maximum on the defect atom. There are four lobes around the P atom which are related to the P-Si bond. From our previous study,[24] we showed that the defect wave function has an overall exponential decay radially from the P atom. For B, we plot the lowest unoccupied wave function in Fig. 1(b). The wave function is asymmetric with a maximum of the wave function on one of the B-Si bond instead of the B atom. This is because B has only three valence electrons. Therefore, one of the four B-Si bonds cannot be satisfied. Li is known to be a very shallow donor in Si. As shown in Fig. 1(c), the Li atom appears ionized and the corresponding defect wave function is more delocalized as a result.

A well-defined measure of the size of the defect wave function $\phi(\mathbf{r})$ can be determined by

$$\langle r\rangle = \int r|\phi(\mathbf{r})|^2 d^3r. \tag{5}$$

Our calculated size is shown in Fig. 2(a) as a function of nanocrystal size. As expected, the Li defect wave function is the most extended among the three dopants while P has the most localized wave function. For the nanocrystals that we studied, $2\langle r\rangle$ is roughly half of the nanocrystal size. For both Li and P, a linear relationship between the two quantities can be observed as well. $\langle r\rangle$ should flatten off and tends to their bulk values for large Si nanocrystals. Since the envelope of the defect wave function has the same functional form as a hydrogen $1s$ orbital, the bulk value can be estimated using a hydrogenic model by $3a_B \times \epsilon/m^*$. a_B=0.529 Å is the hydrogen Bohr radius, ϵ=11.4 is the dielectric constant of bulk Si, and m^*=0.26 is the effective mass of electron in bulk Si. Therefore, $2\langle r\rangle$ should converge approximately to 69.6 Å in the bulk limit, which is not within the span of Fig. 2(a). Assuming a linear relationship between $\langle r\rangle$ and the nanocrystal diameter, the bulk limit can be attained when a Si nanocrystal is ~20 nm in diameter.[24]

We find that the more localized defect wave functions lead to a higher electronic binding energy as depicted in Fig. 2(c). The binding energy is calculated using ΔSCF by Eq. (3) for Li and P donors. For B acceptors, the binding energy is the difference between the electron affinity of a B-doped Si nanocrystal and the ionization energy of a pure Si nanocrystal with the same size. Since the binding energy is dominated by the Coulomb interaction between the dopant ion and the defect electron/hole,[24] the trend in the binding energy is strongly correlated with $\langle 1/r\rangle$ as shown in Fig. 2(b). $\langle 1/r\rangle$ is the expectation value of $1/r$ calculated in a similar manner as in Eq. (5).

B. Strain in doped Si nanocrystal

Given a neutral dopant atom at the center of a Si nanocrystal, we plot the dopant-Si bond length for P and B and the Si-Si bond length adjacent to Li in Fig. 3(a) as a function of nanocrystal size. The P-Si bond length is nearly the same as that of bulk Si; P does not introduce strain to the system. On the contrary, B imposes a huge amount of strain (12–16 %) to the surrounding Si atoms. We also find a Jahn-Teller distortion that lowers the symmetry of the Si nanocrystal from T_d to C_{3v} as the B relaxes along the $\langle 111\rangle$ direction. This results in one of the B-Si bonds longer than the other three equivalent bonds. The longer bond is where the defect wave function is localized in Fig. 1(b). The asymmetry diminishes with increasing nanocrystal size because such distortion becomes energetically unfavorable in a bulk environment. Similar results have also been obtained in Ref. 4. Since Li is located at an interstitial site, the surrounding Si bonds need to be expanded to accommodate the defect atom. The induced strain is ~2% for this case. For both B and Li, the defect-induced strain is only significant within ~4 Å around the dopant.

In order to relate to ΔE^+ or ΔE^-, we need to know the defect-induced strain for an ionized nanocrystal as well. If the defect electron is removed from the P- or Li-doped Si nanocrystals, we find that the bond lengths are changed by less than 0.02 Å. If an electron is added to a B-doped Si nanocrystal, the elongated B-Si bond will be shortened and become equivalent to the other three B-Si bonds. Qualitatively, the amount of strain that a defect ion imposes on its surrounding Si atoms is quite similar to a neutral nanocrystal.

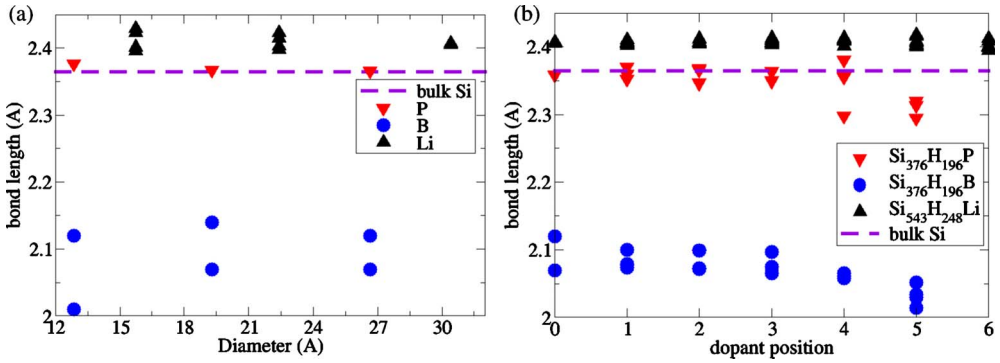

FIG. 3. (Color online) (a) P-Si bond lengths, B-Si bond lengths, and the 12 Si-Si bond lengths around the Li atom as a function of Si nanocrystal size. The dopant atom is at the center of the nanocrystal. (b) The bond lengths for different P and B (Li) position within the Si nanocrystal of diameter 26.6 Å (30.4 Å) in (a).

IV. DEPENDENCE OF TOTAL ENERGY ON DOPANT POSITION

The change in total energy ΔE of a doped Si nanocrystal as a function of the dopant position is shown in Fig. 4. We focus on our largest calculated nanocrystals in Fig. 4(c). The results for the smaller nanocrystals can be understood similarly.

A. Phosphorus

From Fig. 4(c), the total energy depends weakly on the P position.[24] The trend agrees with Ref. 5. Figure 5(a) illustrates the decomposition of ΔE into two components as suggested by Eq. (2). Only ΔE and the change in electronic binding energy $-\Delta BE$ is plotted in the figure, ΔE^{+} is the difference between the two curves. $-\Delta BE$ and ΔE nearly overlap each other if the P atom is more than a bond length away from the surface. The reduction in binding energy can be understood by $\langle 1/|\mathbf{r}-\mathbf{r_d}|\rangle$ in Fig. 5(d), where $\mathbf{r_d}$ is the position of the P atom. The data point for $\mathbf{r_d}=0$ corresponds to the Si nanocrystal having a diameter of 26.6 Å with P at the center in Fig. 2(b). $\langle 1/|\mathbf{r}-\mathbf{r_d}|\rangle$ measures the variation in Coulomb interaction energy between the dopant ion and the defect electron as P changes position. When P moves from the center to the surface of a Si nanocrystal, the system loses Coulomb interaction energy. This is related to $\langle x-x_d\rangle$ in Fig. 5(e), which is the expectation value of x of the defect wave function with respect to the x coordinate of P. As P moves toward the right, i.e., x_d increases, $\langle x-x_d\rangle$ decreases. This implies that the defect wave function does not follow perfectly the P atom but centers to the left of P owing to quantum confinement. As a result, the Coulomb interaction weakens as P gets close to the surface.

When the P is less than a bond length away from the nanocrystal surface, there is substantial contribution from ΔE_i^{+} that counteracts the energy increase from $-\Delta BE$. In Sec. III B, we found that P introduces negligible strain to the nanocrystal. Therefore, it is unlikely that the total energy is lowered by a release of P-induced strain. According to Fig. 3(b), the P-Si bond is contracted and therefore stronger at the surface. This implies an interaction of the P ion with the surface states that lower the surface energy of the Si nanocrystal.

B. Boron

A very different trend can be observed for B-doped Si nanocrystals. From Fig. 4(c), the total energy first increases and then decreases rapidly when the B atom is three bond length away from the surface in agreement with Refs. 4 and 5. Figure 5(b) shows that the system loses electronic binding energy at first but the binding energy increases as the B gets closer to the nanocrystal surface. Such peculiar trend is also observed in Fig. 5(d) as the Coulomb interaction is maximized when the B is either at the center or surface of the

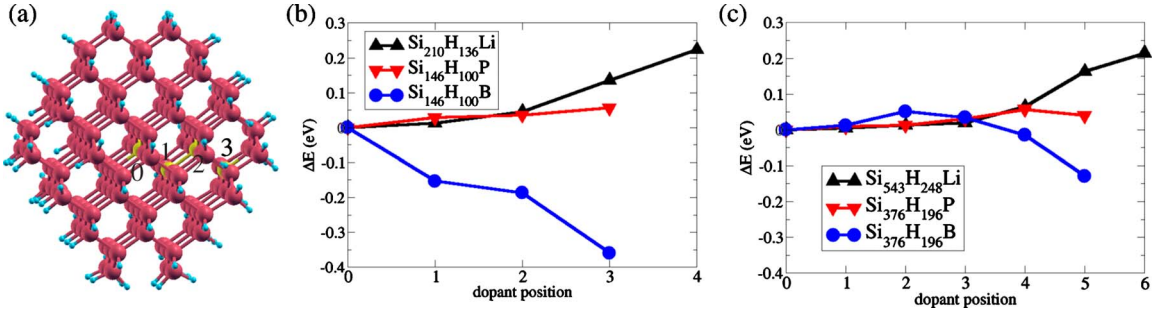

FIG. 4. (Color online) (a) An atomic model of a Si nanocrystal labeling the different positions that will be substituted by a P or B dopant. [(b) and (c)] The variation in total energy of a doped Si nanocrystal as a function of dopant position for nanocrystals with different size. The total energies are with respect to the Si nanocrystal with the dopant at the center.

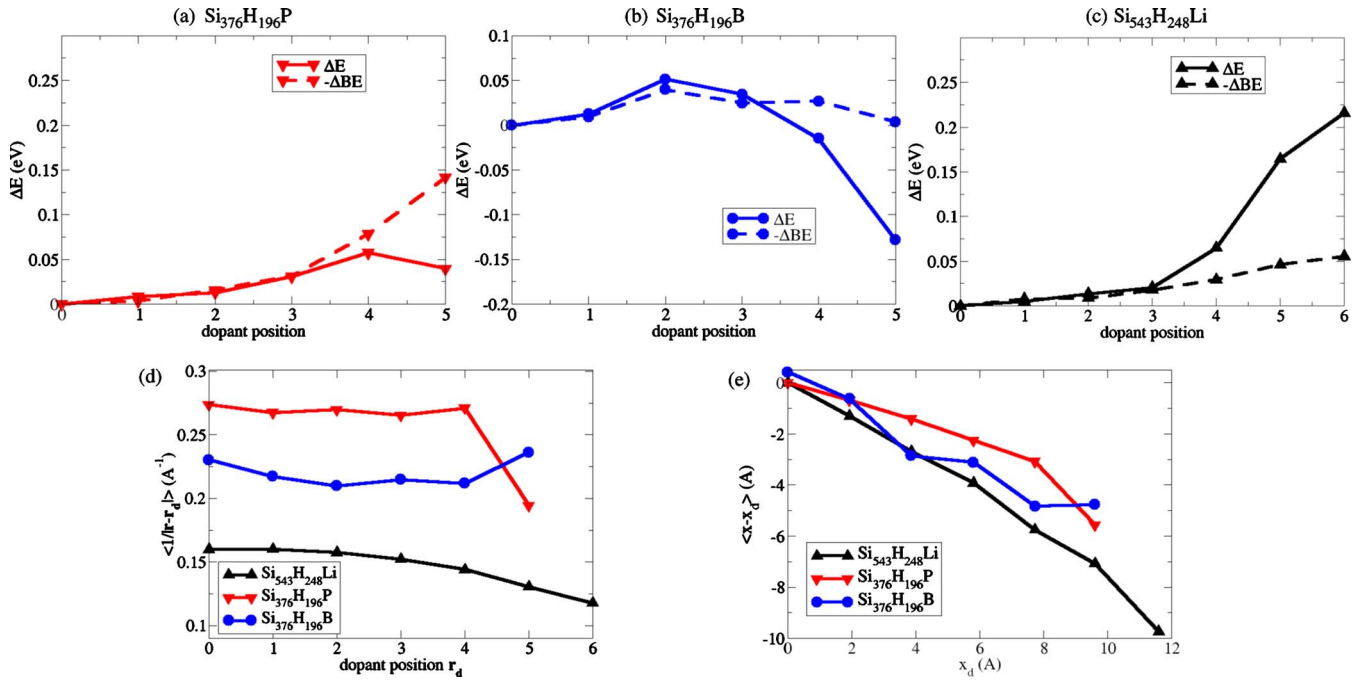

FIG. 5. (Color online) A decomposition of the total-energy variations (ΔE) in Fig. 4(c) according to Eqs. (2) and (4). $-\Delta BE$ is the variation in the electronic binding energy. The difference between ΔE and $-\Delta BE$ corresponds to ΔE^+ for P and Li, or ΔE^- for B. The decomposition is illustrated for (a) P-, (b) B-, and (c) Li-doped Si nanocrystals. The y axis of the three plots all have a span of 0.3 eV, so the height of the plots can be directly compared. (d) A measure of the Coulomb interaction energy ($\langle 1/|\mathbf{r}-\mathbf{r_d}|\rangle$) and (e) the asymmetry of the defect wave function ($\langle x-x_d\rangle$) for different dopant position. $\mathbf{r_d}$ and x_d are the position and the x coordinate of the dopant ion, respectively.

nanocrystal. This behavior is related to the localization of the defect wave function on the elongated B-Si bond. Since one of the four B-Si bonds are slightly elongated, the loss in Coulomb interaction can be compensated by elongating the B-Si bond that is closest to the surface resulting in the defect wave function more centered on the B atom as a whole. This is illustrated in Fig. 6. The elongated B-Si bond points toward the nanocrystal surface and there is a localization of the defect wave function on that bond. A plot of $\langle x-x_d\rangle$ in Fig. 5(e) demonstrates the effect as the curve is no longer monotonically decreasing.

The large drop in total energy close to the surface of the nanocrystal is mostly from ΔE^-. In contrary to P, B induces significant strain to the surrounding Si atoms. From Fig. 3(b), B-Si bonds also become smaller when B moves toward the surface. Therefore, the decrease in total energy can be attributed to a relief of defect-induced strain at the nanocrystal surface as well as a decrease in nanocrystal surface energy.

C. Lithium

The total energy is monotonically increasing as the Li atom moves from the center toward the surface. As shown in Fig. 5(c), the initial increase occurs because of a decrease in electronic binding energy. While the binding energy continues to decrease as Li gets closer to the surface, the total energy increase is significantly larger. Since Li has an extended defect wave function, it is expected that the binding energy should be more susceptible to the effect of quantum confinement. As illustrated by $\langle x-x_d\rangle$ in Fig. 5(e), the defect wave function is more deformed and off-centered from the Li ion when it moves toward the surface. However, the decrease in binding energy is only 0.05 eV at the surface compared to 0.14 eV for P. This occurs because the Li defect wave function does not have a maximum on the Li position as shown in Fig. 1(c), and Fig. 5(d) shows that the reduction in Coulomb interaction is relatively small at the surface. In contrast, if the maximum of the defect wave function is localized on the dopant as in P, the loss in Coulomb energy as the dopant moves toward the surface should be significantly larger.

Since $-\Delta BE$ can only account for approximately one third of the total energy increase at the surface, the rest is from ΔE^+. The Si bonds at the surface of a H-passivated Si nanocrystal with no defects are slightly contracted compared to the bulk, while Figs. 3(a) and 3(b) show that interstitial Li causes the surrounding Si bonds to expand, this increases the surface energy of the nanocrystal and ΔE^+.

D. Small nanocrystals

For smaller Si nanocrystals, our calculated variation in total energy with dopant position is shown in Fig. 4(b). The Li shows a similar trend as in the larger nanocrystal, and the position dependence remains weak for P. For B-doped nanocrystals smaller than 2 nm in diameter, the energy minimum at the center of the nanocrystal vanishes. This follows from our results of the larger nanocrystal that B three bond lengths away from the surface starts to show a decrease in total energy.

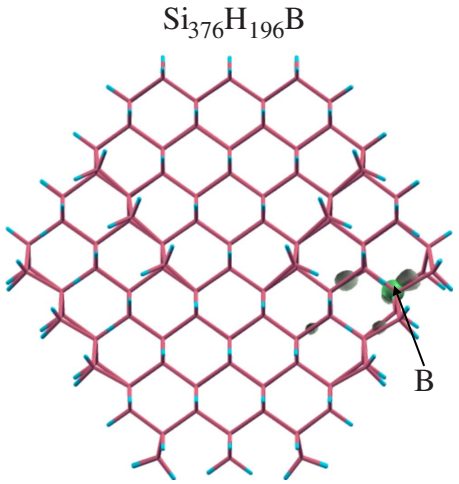

FIG. 6. (Color online) A surface contour plot of the defect wave function for a B-doped Si nanocrystal with the B atom close to the surface. The B atom is labeled in the figure.

V. CONCLUSION

We examined the change in total energy of a doped Si nanocrystal as a function of dopant position by decomposing the total energy variation into two terms: the change in the electronic binding energy and a surface term related to the interaction between the dopant and the nanocrystal surface. For both P and Li, the binding energies decrease when the dopant moves toward the surface owing to a loss of Coulomb interaction energy between the dopant ion and the defect electron. While expelling a P defect helps to lower the nanocrystal surface energy, the interstitial Li ion induces significant strain and increases the surface energy. This leads to a weak position dependence of the total energy for P because of the two compensating contributions while Li has a strong tendency to stay inside the nanocrystal core because both contributions act in the same direction. For B, there is a bistable behavior for nanocrystals larger than 2 nm in diameter. The energy minimum at the center of the nanocrystal comes from the binding energy contribution. Close to the surface, strain relief is the dominant factor leading to a drop in total energy.

For all the three dopants, the electronic binding energy contribution leads to a local minimum of the total energy at the nanocrystal center. We predict that if a shallow dopant can diffuse 2–3 atomic layers into the surface of a nanocrystal, the dopant will tend to move toward the nanocrystal core thus avoiding self-purification, unless the nanocrystal is smaller than ~2 nm in diameter. Our study reveals that the surface terms ΔE^+ and ΔE^- depend on the detailed chemistry of the dopants, and probably on the nanocrystal passivation as well. From the energetics perspective, since the core of a nanocrystal is always an energy minimum, self-purification is governed by whether there is an energy minimum or maximum close to the nanocrystal surface, which can be manipulated by using different surface passivation or modifying the surface reconstruction.

ACKNOWLEDGMENTS

The work was supported in part by the U.S. Department of Energy, Office of Basic Energy Sciences under Grant No. DE-FG02-06ER46286. Computational work was supported by the National Science Foundation under Grant No. DMR 09-41645. Work at Rensselaer Polytechnic Institute was supported by the U.S. Department of Energy under Contract No. DE-SC0002623. Computational resources were provided in part by the National Energy Research Scientific Computing Center (NERSC), the Texas Advanced Computing Center (TACC), and the Computational Center for Nanotechnology Innovations (CCNI).

[1] F. V. Mikulec, M. Kuno, M. Bennati, D. A. Hall, R. G. Griffin, and M. G. Bawendi, J. Am. Chem. Soc. **122**, 2532 (2000).
[2] S. C. Erwin, L. Zu, M. I. Haftel, A. L. Efros, T. A. Kennedy, and D. J. Norris, Nature (London) **436**, 91 (2005).
[3] G. M. Dalpian and J. R. Chelikowsky, Phys. Rev. Lett. **96**, 226802 (2006).
[4] G. Cantele, E. Degoli, E. Luppi, R. Magri, D. Ninno, G. Iadonisi, and S. Ossicini, Phys. Rev. B **72**, 113303 (2005).
[5] Q. Xu, J.-W. Luo, S.-S. Li, J.-B. Xia, J. Li, and S.-H. Wei, Phys. Rev. B **75**, 235304 (2007).
[6] J. Li, S.-H. Wei, S.-S. Li, and J.-B. Xia, Phys. Rev. B **77**, 113304 (2008).
[7] T.-L. Chan, A. T. Zayak, G. M. Dalpian, and J. R. Chelikowsky, Phys. Rev. Lett. **102**, 025901 (2009).
[8] C. K. Chan, H. Peng, K. McIlwrath, X. F. Zhang, R. A. Huggins, and Y. Cui, Nat. Nanotechnol. **3**, 31 (2008).
[9] P. Hohenberg and W. Kohn, Phys. Rev. **136**, B864 (1964).
[10] W. Kohn and L. J. Sham, Phys. Rev. **140**, A1133 (1965).
[11] J. R. Chelikowsky, N. Troullier, and Y. Saad, Phys. Rev. Lett. **72**, 1240 (1994).
[12] J. R. Chelikowsky, J. Phys. D **33**, R33 (2000).
[13] PARSEC has a website at http://parsec.ices.utexas.edu
[14] Y. Zhou, Y. Saad, M. L. Tiago, and J. R. Chelikowsky, Phys. Rev. E **74**, 066704 (2006).
[15] Y. Zhou, Y. Saad, M. L. Tiago, and J. R. Chelikowsky, J. Comput. Phys. **219**, 172 (2006).
[16] D. M. Ceperley and B. J. Alder, Phys. Rev. Lett. **45**, 566 (1980).
[17] J. P. Perdew and Y. Wang, Phys. Rev. B **45**, 13244 (1992).
[18] N. Troullier and J. L. Martins, Phys. Rev. B **43**, 1993 (1991).
[19] L. Kleinman and D. M. Bylander, Phys. Rev. Lett. **48**, 1425 (1982).
[20] M. Fujii, K. Toshikiyo, Y. Takase, Y. Yamaguchi, and S. Hayashi, J. Appl. Phys. **94**, 1990 (2003).
[21] Y. Tu and J. Tersoff, Phys. Rev. Lett. **84**, 4393 (2000).
[22] We also tested the possibility of interstitial P in Si nanocrystals. We compare the formation energies of substitutional and interstitial P using a small $Si_{35}H_{36}$ nanocrystal (diameter 13 Å). For substitutional P, the formation energy depends on the Si chemical potential μ(Si) after the replaced Si atom is extracted from the nanocrystal. Our study shows that μ(Si) needs to be higher

than −7.58 Ry in order for the formation of interstitial P to be energetically favorable compared to substitutional P. According to our calculations, the total energy of bulk Si is −7.93 Ry/atom, which is 4.77 eV lower than our calculated lower bound. If the extracted Si atom is deposited into a bulklike environment, it is highly unlikely that interstitial P can be formed in the nanoregime even if the P atom is close to the surface. We reach the same conclusion for the comparison between substitutional and interstitial B.

[23] R. O. Jones and O. Gunnarsson, Rev. Mod. Phys. **61**, 689 (1989).

[24] T.-L. Chan, M. L. Tiago, E. Kaxiras, and J. R. Chelikowsky, Nano Lett. **8**, 596 (2008).